

Nanotribology and Nanoscale Friction

YI GUO, ZHIHUA QU, YEHUDA BRAIMAN,
ZHENYU ZHANG, and JACOB BARHEN

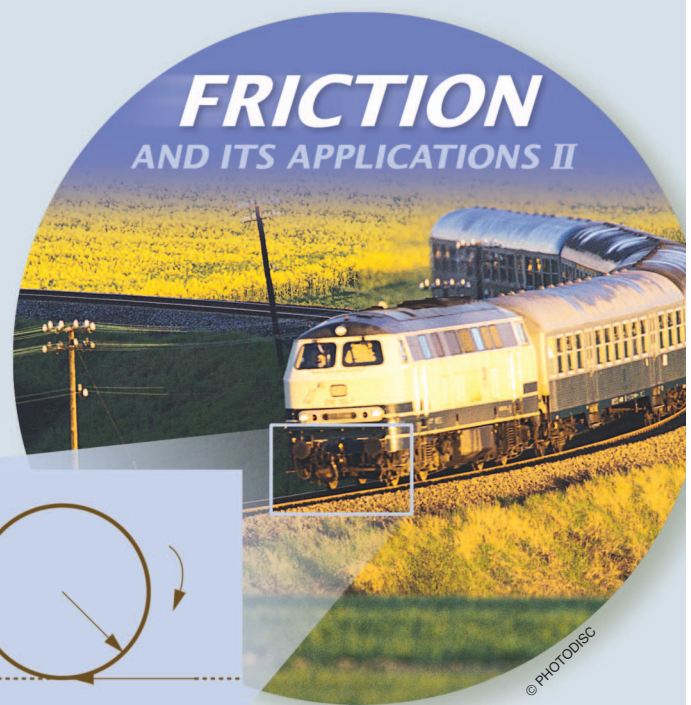
SMOOTH SLIDING THROUGH FEEDBACK CONTROL

Tribology is the science and technology of contacting solid surfaces in relative motion, including the study of lubricants, lubrication, friction, wear, and bearings. It is estimated that friction and wear cost the U.S. economy 6% of the gross national product [1]. For example, 5% of the total energy generated in an automobile engine is lost to frictional resistance. The study of nanoscale friction has a technological impact in reducing energy loss in machines, in microelectromechanical systems (MEMS), and in the development of durable, low-friction surfaces and ultra-thin lubrication films.

Friction between contacting surfaces is a longstanding and crucially important scientific problem, which is characterized by the interplay of energy, stress, and chemistry at many length scales. To understand friction and to meet technology needs, knowledge from the fields of chemistry, material science, physics, mathematics, and engineering must be applied. Fundamental scientific questions include how energy is dissipated in nonequilibrium processes and how the course of energy dissipation can be intentionally controlled. The road map between friction, which is an ensemble-averaged quantity, and molecular-level dynamics remains open. These issues are relevant to the development of energy-efficient technologies, such as ultra-thin lubricant films for ultra-high-temperature lubrication as well as for control and manipulation of frictional properties during sliding.

Friction is intimately related to both adhesion and wear, which are nonequilibrium, multiscale phenomena, from the atomic level to the molecular level to the microscopic level.

Digital Object Identifier 10.1109/MCS.2008.929420



As such, multidisciplinary studies are required to reveal the nature of sliding on a variety of surfaces (smooth or rough; elastic, viscoelastic, or plastic; dry or lubricated) that possess different types of chemistry. Some of the outstanding issues and questions are the following:

- » experimental and theoretical elucidation of the linear characteristics of friction at or near an equilibrium and their relation to statistical-mechanical theories of solids and liquids at equilibrium

- » elucidation of the nonlinear characteristics of friction away from an equilibrium and their relation to theories of complexity and modern computational resources
- » development of theory beyond empiricism that can explain and predict why lubricating molecules of one chemical structure are more effective than others in lowering friction forces
- » design of tribological surfaces with desired frictional properties, that is, principles for surface engineering, as well as control of frictional properties during sliding in order to achieve desired friction characteristics
- » friction and lubrication under extreme conditions, such as high-temperature or nonequilibrium, including phenomena such as stick-slip boundary conditions at the macroscale, triboluminescence, and quantum effects in tribology.

In light of these challenges, our focus in this article is on modeling and control of friction so that the closed-loop frictional dynamics produce a desired motion. In particular, we describe the model systems, formulate a control problem, present two control strategies, and conduct detailed analyses of single-particle dynamics in both the open-loop and closed-loop systems.

FRICION CONTROL AT THE NANOSCALE

Sliding friction can be significantly reduced or increased by applying small perturbations [2]–[9]. The effect of small perturbations on frictional dynamics is a consequence of the highly nonlinear nature of this phenomenon. A wide variety of stable and unstable equilibria may exist depending on the system parameters. Using a surface-force apparatus modified to measure friction forces while inducing normal (perpendicular to the surface) vibrations of one of the sliding surfaces, load- and frequency-dependent transitions between various dynamical friction states can be observed [4]. Moreover, these observations reveal regimes of extremely low friction, which is highly desirable for many applications. The effect of periodic and random surface oscillations on frictional properties is studied in [7]–[9] using an atomic force microscope (AFM). Since [10], the AFM has been widely used to mea-

sure frictional properties of materials at the atomic scale [11], [12]. As in the surface-force apparatus experiment [4], a significant reduction in the friction force and extremely low friction are observed when one of the sliding surfaces is subjected to small amplitude oscillations, both normal (perpendicular to the sliding surfaces) and lateral (parallel to the sliding surfaces) [6], [8], [9], [13]. In addition, surface roughness and thermal noise due to vibrations of the atoms on the surface are expected to play a significant role in the development of control strategies at the micro and nanoscales [14], [15].

Despite experiments in support of theoretical modeling, fundamental questions on how to control friction are open [16]. In this article, two types of feedback controllers, namely, non-Lipschitzian control [17] and Lyapunov-based control, are investigated. We show that the friction force can be significantly reduced using feedback control. With the help of nonlinear control theory, closed-loop stability is analyzed and subsequently verified using numerical simulations. The frictional dynamics are assumed to be described by the Frenkel-Kontorova (FK) model, which is the subject of the next section.

THE FRENKEL-KONTOROVA MODEL

The Frenkel-Kontorova model describes the dynamics of a chain of particles, whose interactions are between the nearest neighbors and are subjected to an external potential. The complexity of this model, which can be used as a general framework for describing friction [1], ranges from a simplified one-dimensional model, to two- and three-dimensional models, and finally, to a full set of molecular equations. In addition, the FK model is applied in [18] to various physical systems, including sliding friction, charge-density waves, magnetic spirals, and adsorbed monolayers.

As reviewed in [18], the FK model can be traced back to the model studied by Prandtl and Dehlinger in 1928 and 1929. This model, which was independently introduced by Frenkel and Kontorova in 1938, can be derived for the chain of particles depicted in Figure 1. The equation of motion for this one-dimensional array of N identical particles moving on a surface can be derived from Newton's laws of motion as [18]

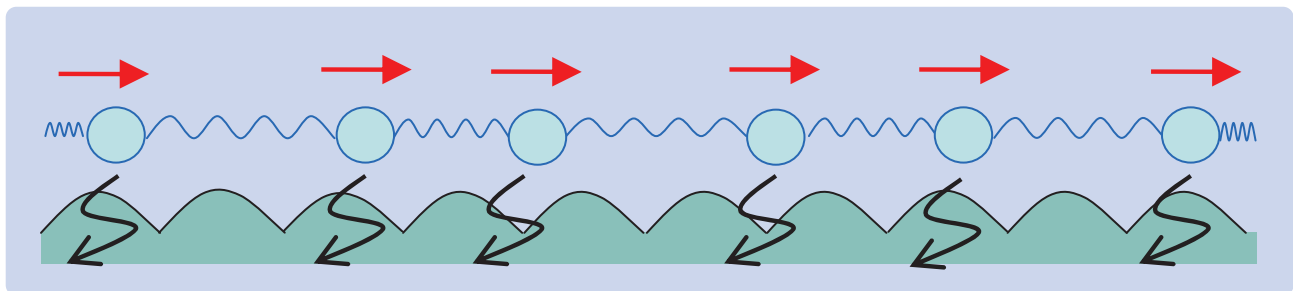


FIGURE 1 The Frenkel-Kontorova model. This model describes a harmonic chain (mimicking a layer of nanoparticles) in a spatially periodic potential (mimicking the substrate). The chain is driven by a constant force, and the dynamics are damped by a velocity-proportional damping.

$$m\ddot{x}_i + \gamma' \dot{x}_i = -\frac{\partial U(x_i)}{\partial x_i} - \frac{\partial W(x_i - x_j)}{\partial x_i} + f' + \eta(t), \quad i = 1, \dots, N, \quad (1)$$

where x_i is the displacement of the i th particle, m is the mass of each particle, $\gamma' > 0$ is the friction coefficient characterizing the energy exchange between a single particle and the substrate, f' is the externally applied force, $\eta(t)$ is the thermal noise forcing, $U(x_i)$ is the potential applied by the substrate, and $W(x_i - x_j)$ is the particle-interaction potential. These potentials arise from various physical origins, such as the van der Waals potential [19].

We assume that the substrate potential is spatially periodic and has the form

$$U(x_i) = \frac{1}{2}\Phi \sum_{i=1}^N \left(1 - \cos \frac{2\pi x_i}{a}\right), \quad (2)$$

where $\Phi > 0$ is an energy constant, and $a > 0$ is the period. The particle-interaction potential is assumed to take the form

$$W(x_i - x_j) = \frac{1}{2}K \sum_{i=1}^{N-1} (x_{i+1} - x_i - b)^2, \quad (3)$$

where $K > 0$ is a constant, and b is the equilibrium interatomic distance. We further assume that the same force is applied to each particle and that the noise is absent, hence $\eta(t) = 0$. Defining the dimensionless phase variable $z_i = (2\pi x_i/a)$ and dimensionless time $\tau = \sqrt{(2\Phi/m)}(\pi/a)t$, the equation of motion (1) reduces to the dimensionless simplified FK model [18], [20]

$$\ddot{z}_i + \gamma \dot{z}_i + \sin(z_i) = f + F_i, \quad (4)$$

where $\gamma = (\gamma' a^2 / \sqrt{2m\Phi\pi^2})$, $f = (f' a / \pi \Phi)$, $\kappa = (K a^2 / 2\Phi\pi^2)$, and F_i is the nearest neighbor interaction force, which has the form

$$F_i = \kappa(z_{i+1} - 2z_i + z_{i-1}), \quad i = 2, \dots, N-1, \quad (5)$$

with the free-end boundary conditions

$$F_1 = \kappa(z_2 - z_1), \quad F_N = \kappa(z_{N-1} - z_N). \quad (6)$$

Various experimental techniques are used to gain fundamental insights into friction. These techniques include the surface-force apparatus (SFA), quartz-crystal microbalance (QCM), and AFM. The FK model is applicable to QCM experiments, where a one- or two-dimensional system of interacting atoms slides over the periodic substrate potential.

CONTROL PROBLEM FORMULATION

Control at the nanoscale presents many challenges. Due to strict confinement and additional constraints,

nanosystems are not readily accessible and not all particles can be targeted or controlled individually. For the nanoparticle system, the accessible quantities include the position z_{cm} and velocity v_{cm} of the center of mass of the particles given by

$$v_{\text{cm}} = \frac{1}{N} \sum_{i=1}^N \dot{z}_i, \quad z_{\text{cm}} = \frac{1}{N} \sum_{i=1}^N z_i.$$

A control variable $u(t)$ representing a dimensionless external force is added to the system model (4) to obtain, for $i = 1, \dots, N$, [20]

$$\ddot{z}_i + \gamma \dot{z}_i + \sin(z_i) = f + F_i + u(t). \quad (7)$$

As a feedback control, $u(t)$ can be a function of only the accessible quantities v_{cm} and z_{cm} . The control problem based on the model (4) is thus to design a feedback control law of the form

$$u = u(v_{\text{target}}, v_{\text{cm}}, z_{\text{cm}}), \quad (8)$$

such that v_{cm} tends to v_{target} , where v_{target} is the constant commanded velocity of the center of mass of the particles.

Without the control term $u(t)$, (7) can exhibit complex dynamics, including rest, periodic stick-slip, chaotic stick-slip, and periodic sliding [20]. The control objective is to achieve smooth sliding of the system so that the effects of dynamic friction are reduced.

FEEDBACK CONTROL STRATEGIES

Several feedback control strategies are studied in the literature for the control problem formulated above [20], [21]. Here, we describe and compare two representative schemes.

Non-Lipschitzian Control

The feedback control algorithm considered in [20] is based on the concept of a terminal attractor, which is usually associated with non-Lipschitzian dynamics. The non-Lipschitzian control law is given by

$$u(t) = \beta(v_{\text{target}} - v_{\text{cm}}(t))^\xi, \quad (9)$$

where β is a positive constant, $\xi = 1/(2n + 1)$, and n is a positive integer. The form of ξ ensures that (9) has a real solution.

The control law (9) causes the velocity of the center of mass v_{cm} to converge to the targeted value v_{target} in finite time. These properties can be illustrated using the concept of terminal attractor [22], [23]. For instance, for $\xi = 1/7$, the control has the equivalent gain

$$\frac{du(t)}{dv_{\text{cm}}(t)} = -\frac{1}{7}\beta(v_{\text{target}} - v_{\text{cm}}(t))^{-\frac{6}{7}}, \quad (10)$$

which approaches $-\infty$ as v_{cm} tends to v_{target} . This “infinite attraction power” of the non-Lipschitzian attractor makes it possible to achieve finite-time convergence [24], [17].

When the commanded velocity v_{target} is close to the average velocity of the center of mass of the particles in an uncontrolled system, the control law (9) may drive the system to the average velocity of the uncontrolled system instead of v_{target} . To achieve the commanded velocity of the center of mass, the control (9) is modified in [20] as

$$u(t) = \beta(v_{\text{target}} - v_{\text{cm}}(t))^{\xi} - \rho(v_{\text{av}}(t) - v_{\text{cm}}(t))^{\xi} \text{sgn}((v_{\text{av}}(t) - v_{\text{cm}}(t))(v_{\text{cm}}(t) - v_{\text{target}}))H[r - \|v_{\text{target}} - v_{\text{av}}(t)\|], \quad (11)$$

where $v_{\text{av}}(t)$ is the running average of $v_{\text{cm}}(t)$, that is, $v_{\text{av}}(t) = (1/t) \int_0^t v_{\text{cm}}(\tau) d\tau$, and $H(\cdot)$ denotes the unit step function. The second term in (11) is a repelling force, which drives the trajectory toward the commanded velocity. This effect of the controller is illustrated by the simulation results shown in the next section.

The control (11) provides a feedback scheme for stabilizing the system (7). Numerical simulations show that this controller has the advantage of fast response time with small control effort. On the other hand, its disadvantages are that it can attract the velocity to only a vicinity of the commanded value and that persistent fluctuations may be present, as shown in the simulation results of the next section.

Control Design Using Lyapunov Stability Methods

Motivated by [20], a smooth control is designed in [21] using Lyapunov’s direct method. Define the tracking-error variables

$$e_{i1} = \dot{z}_i - v_{\text{target}} t, \quad e_{i2} = \dot{z}_i - v_{\text{target}}, \quad (12)$$

and the average tracking-error variables

$$e_{1\text{av}} = z_{\text{cm}} - v_{\text{target}} t, \quad e_{2\text{av}} = v_{\text{cm}} - v_{\text{target}}. \quad (13)$$

Then, the dynamics of the averaged tracking-error system can be written as

$$\dot{e}_{1\text{av}} = e_{2\text{av}} \quad (14)$$

$$\dot{e}_{2\text{av}} = -\frac{1}{N} \sum_{i=1}^N \sin(e_{i1} + v_{\text{target}} t) - \gamma(e_{2\text{av}} + v_{\text{target}}) + u(t). \quad (15)$$

Note that the particle-interaction terms $F_i(\cdot)$ are canceled in (14) and (15).

It is shown in [21] that a smooth feedback control for the average-error system is given by

$$u(t) = -f + \gamma v_{\text{target}} - k_1(z_{\text{cm}} - v_{\text{target}} t) - k_2(v_{\text{cm}} - v_{\text{target}}) + \sin(v_{\text{target}} t), \quad (16)$$

where k_1 and k_2 are positive constants. The control law (16) is synthesized through stability analysis of the closed-loop system using Lyapunov theory. That is, considering the quadratic Lyapunov-function candidate

$$V(t, e_{\text{av}}) = \frac{1}{2} e_{1\text{av}}^2 + \frac{1}{2} (c_1 e_{1\text{av}} + e_{2\text{av}})^2, \quad (17)$$

where $c_1 > 0$, it follows that, under the control law (16), the time derivative of V along the trajectory of the closed-loop average dynamics satisfies

$$\dot{V} \leq -c_1 [e_{1\text{av}}^2 + c_1 (e_{1\text{av}} + e_{2\text{av}})^2] + \frac{1}{c_2}, \quad (18)$$

where c_1 and c_2 are related to the control parameters k_1 and k_2 by

$$k_1 = c_1^2 + c_1 c_2 + 1, \quad k_2 = 2c_1 + c_2 - \gamma. \quad (19)$$

Note that c_1 and c_2 can be adjusted through the selection of k_1 and k_2 and that (18) is negative definite for large values of the tracking errors. The inequality (18) guarantees that the average-error states $e_{1\text{av}}$ and $e_{2\text{av}}$ are uniformly bounded [25], [26]. Further analysis of the inequality (18) provides an ultimate bound b on $e_{1\text{av}}$ and $e_{2\text{av}}$ given by [27]

$$b = \sqrt{\frac{\lambda_{\max}(P)}{c_1 c_2 \lambda_{\min}^2(P)}}, \quad (20)$$

where $\lambda_{\max}(P)$ and $\lambda_{\min}(P)$ are the maximum and minimum eigenvalues of P , respectively, and P is the positive-definite matrix defined by

$$P = \begin{bmatrix} 1 + c_1^2 & c_1 \\ c_1 & 1 \end{bmatrix}.$$

Note that there is a tradeoff between the size of the ultimate bound and the control effort, while tracking errors for the average system become smaller than the ultimate bound after a finite time.

To make the error state $(e_{1\text{av}}, e_{2\text{av}})$ converge to zero, the control law (16) can be modified as

$$u = -f + \gamma v_{\text{target}} - k_1(z_{\text{cm}} - v_{\text{target}} t) - k_2(v_{\text{cm}} - v_{\text{target}}) + \sin(v_{\text{target}} t) - 2\text{sgn}(\xi), \quad (21)$$

where $\text{sgn}(\xi)$ is the signum function defined as $\text{sgn}(\xi) = 1$ for $\xi > 0$, $\text{sgn}(\xi) = -1$ for $\xi < 0$, and $\text{sgn}(\xi) = 0$ for $\xi = 0$. With the switching term $2\text{sgn}(\xi)$ in (21), the time derivative of the Lyapunov function is negative definite, which ensures asymptotic stability of the zero solution of the closed-loop system. Note that the control (21) is again non-Lipschitzian.

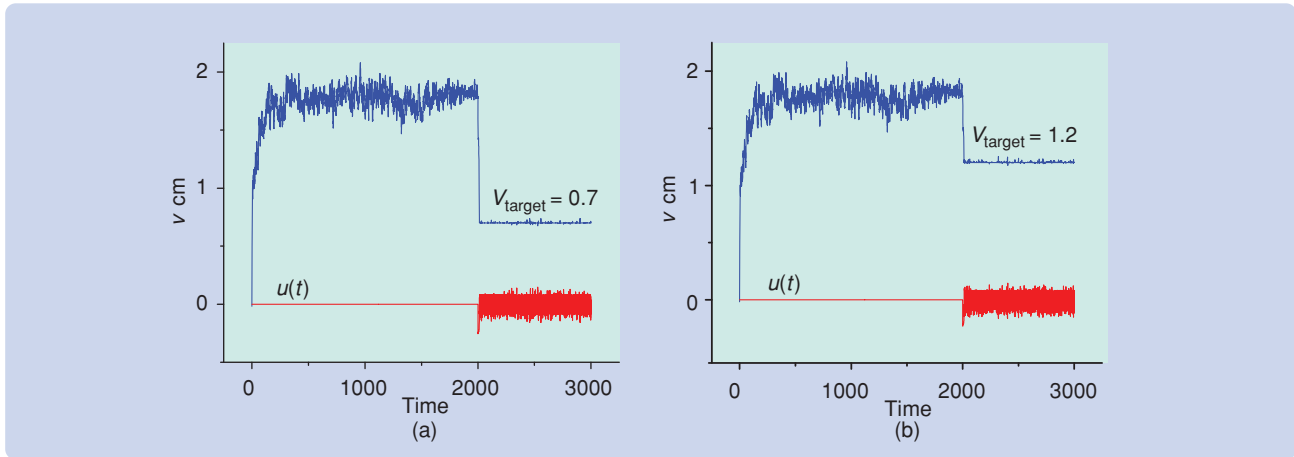


FIGURE 2 Performance of the non-Lipschitzian control (11) for a 128-particle system. Control is initiated at $t = 2000$. The blue lines show the time series of the center-of-mass velocities, while the red lines show the control input. The parameters are $\gamma = 0.1$, $\kappa = 0.26$, $f = 0.3$, $\alpha = 0.25$, and $\xi = 1/7$. All of the quantities are dimensionless.

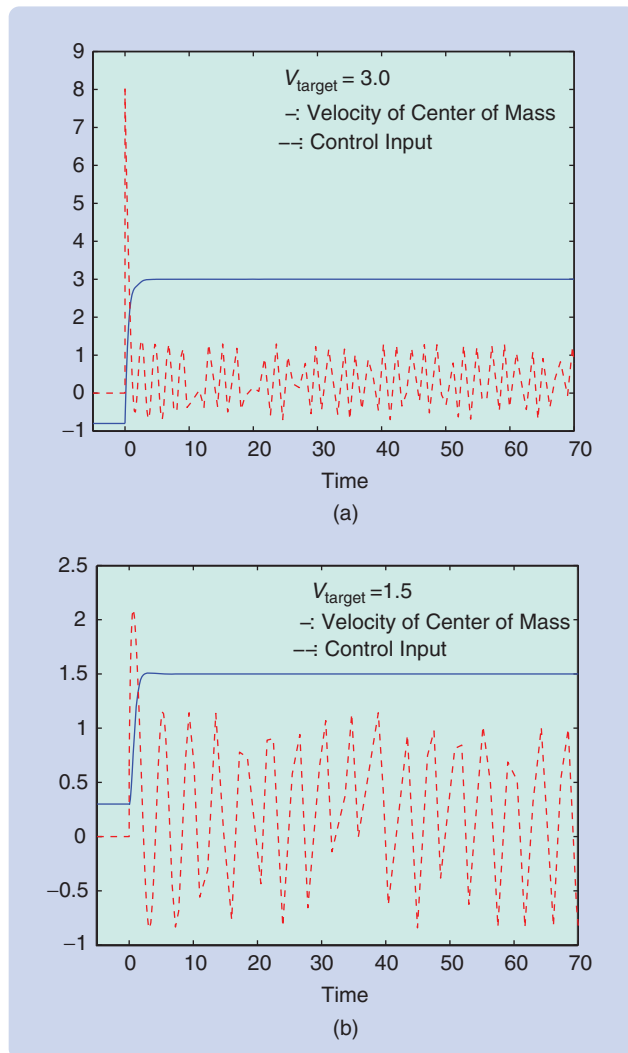


FIGURE 3 Performance of the Lyapunov-based control (16) for a 15-particle system. Control is initiated at $t = 0$. The commanded values are (a) 3.0 and (b) 1.5. The parameters are $\gamma = 0.1$, $\kappa = 0.26$, $f = 0$, $k_1 = 5.07$, and $k_2 = 4.7$.

The Lyapunov argument outlined above provides a systematic design method for synthesizing stabilizing control laws. Control laws (16) and (21) guarantee ultimate boundedness and asymptotic stability of the error state, respectively. The control parameters are directly related to the system performance, and precise control can be achieved. In contrast, switching control can cause chattering along the switching surface [28].

CHARACTERIZATION OF CONTROL PERFORMANCE

Numerical simulations are performed for the non-Lipschitzian and Lyapunov-based controllers. For the non-Lipschitzian control (11), Figure 2 shows the convergence of the velocity of the center of the mass to several commanded values. Persistent oscillations are present, while the amplitude of the control is relatively small compared to the control law shown in Figure 3.

Figure 3 shows the performance of the Lyapunov-based control (16). It can be seen that, with the price of higher control effort, oscillations are eliminated.

Since the objective of the control is to achieve the constant velocity v_{target} , the increase in kinetic energy of the system (7) is $(1/2)mv_{\text{target}}^2$. Figures 2 and 3 show that the time average of the control is close to zero, which indicates the level of energy spent to sustain the kinetic energy.

ANALYSIS OF SINGLE-PARTICLE DYNAMICS

Since the average position and velocity of the center of mass are considered in the control design, the motion of the individual particles must be considered. We first investigate the open-loop stability properties of the particles.

Local Stability of Open-Loop Systems

It follows from (4) that the equilibrium positions of the individual particles without external force ($f = 0$) are given by

$$z_i = l_i \pi, \quad \dot{z}_i = 0, \quad l_i = 0, \pm 1, \pm 2, \dots \quad (22)$$

Since $f = 0$, (4) can be expressed in the state-space form

$$\dot{x}_{i1} = x_{i2}, \quad (23)$$

$$\dot{x}_{i2} = -\sin x_{i1} - \gamma x_{i2} + F_i, \quad (24)$$

where $i = 1, 2, \dots, N$, $x_{i1} = z_i$, $x_{i2} = \dot{z}_i$, and F_i is the nearest neighbor interaction force.

Linearizing (24) around its equilibrium points $(x_{i1}, x_{i2}) = (l_i \pi, 0)$ and stacking all of the state-space equations yields the state-space model

$$\dot{x} = Ax + BFx, \quad (25)$$

where $x = [x_{11} - l_1 \pi \quad x_{12} \quad x_{21} - l_2 \pi \quad x_{22} \quad \dots \quad x_{N1} - l_N \pi \quad x_{N2}]^T$,

$$A = I_N \otimes A_p, \quad B = I_N \otimes B_p, \quad F = Q \otimes [\kappa \quad 0], \quad (26)$$

$$A_p = \begin{cases} \begin{bmatrix} 0 & 1 \\ -1 & -\gamma \end{bmatrix}, & \text{for } l_i = 2k\pi, k = 0, \pm 1, \dots, \\ \begin{bmatrix} 0 & 1 \\ 1 & -\gamma \end{bmatrix}, & \text{for } l_i = (2k+1)\pi, \end{cases} \quad (27)$$

$$B_p = \begin{bmatrix} 0 \\ 1 \end{bmatrix}, \quad Q = \begin{bmatrix} -1 & 1 & 0 & \dots & 0 \\ 1 & -2 & 1 & 0 & \dots \\ & & \vdots & & \\ 0 & \dots & 1 & -2 & 1 \\ 0 & \dots & 0 & 1 & -1 \end{bmatrix}, \quad (28)$$

\otimes is the Kronecker product, and I_N is the $N \times N$ identity matrix.

It follows from

$$\begin{aligned} BF &= (I_N \otimes B_p) (Q \otimes [\kappa \quad 0]) \\ &= (I_N Q) \otimes (B_p [\kappa \quad 0]) = Q \otimes \begin{bmatrix} 0 & 0 \\ \kappa & 0 \end{bmatrix} \end{aligned}$$

that all of the eigenvalues of BF are zero. In fact, the linearized system (25) includes coupling between the neighboring particles. Connectivity of the particles can be described by the bidirectional graph shown in Figure 4, whose Laplacian matrix [29] is $-Q$. Recall that the Laplacian matrix L_G is defined by $L_G = D - A$, where A is the adjacency matrix with diagonal entries zero and off-diagonal entries $a_{ij} = 1$ if there is a link from node i to node j , otherwise $a_{ij} = 0$; D is the degree matrix with diagonal entries $d_{ii} = \sum_{j=1}^n a_{ij}$ and off-diagonal entries 0.

It can be seen that each isolated subsystem has an asymptotically stable equilibrium at $(2k\pi, 0)$ and an unstable equilibrium at $((2k+1)\pi, 0)$. In fact, without particle interaction, (24) becomes that of a damped pendulum equation, where the equilibrium $(2k\pi, 0)$ corresponds to the asymptotically stable downward position, and the

It is estimated that friction and wear cost the U.S. economy 6% of the gross national product.

equilibrium $((2k+1)\pi, 0)$ corresponds to the unstable upward position [25]. The question naturally arising is whether the stability properties are the same in the presence of particle interactions.

To answer this question, we examine the matrix $A + BF$ in (25). Since A is block diagonal, we use a similarity transformation to make $A + BF$ block diagonal. Since Q is symmetric, there exists an orthogonal transformation matrix T such that $T^{-1}QT = D$, where D is a diagonal matrix of eigenvalues of Q . Hence,

$$(T \otimes I_2)^{-1} (BF) (T \otimes I_2) = D \otimes \begin{bmatrix} 0 & 0 \\ \kappa & 0 \end{bmatrix}. \quad (29)$$

Block diagonalization (29) can be used to determine stability. Q is a row-sum-zero matrix all of whose off-diagonal entries are negative, and $-Q$ is positive semidefinite. It follows that the eigenvalues of Q satisfy [29], [30]

$$\mu_1 \leq \mu_2 \leq \dots \leq \mu_{N-1} \leq \mu_N = 0. \quad (30)$$

Consequently, the diagonal matrix D has nonpositive diagonal entries. Since

$$\begin{aligned} (T \otimes I_2)^{-1} A (T \otimes I_2) &= (T^{-1} I_N T) \otimes (I_2 A_p I_2) \\ &= I_N \otimes A_p = A, \end{aligned} \quad (31)$$

it follows that

$$(T \otimes I_2)^{-1} (A + BF) (T \otimes I_2) = H, \quad (32)$$

where H is the block diagonal matrix with diagonal entries

$$H_{ii} = \begin{cases} \begin{bmatrix} 0 & 1 \\ -1 + \mu_{i\kappa} & -\gamma \end{bmatrix}, & \text{at equilibrium } (2k\pi, 0), \\ \begin{bmatrix} 0 & 1 \\ 1 + \mu_{i\kappa} & -\gamma \end{bmatrix}, & \text{at equilibrium } ((2k+1)\pi, 0). \end{cases} \quad (33)$$

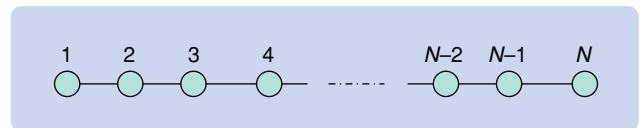


FIGURE 4 Connectivity of the particles. This bidirectional graph shows a nearest neighbor structure, whose Laplacian matrix is strongly connected. The property is used to establish local stability of the open-loop system.

**Despite experiments in support of theoretical modeling,
fundamental questions on how to control friction are open.**

It follows from (30) that H has negative eigenvalues at the equilibrium $(2k\pi, 0)$ and at least one positive eigenvalue at others. We thus conclude that, in the absence of external forces, the particle array is asymptotically stable at $(2k\pi, 0)$ and unstable at $((2k+1)\pi, 0)$ with and without particle interactions.

**Stability of Single Particles
in the Closed-Loop Tracking System**

After the discussion on open-loop stability, we turn our attention to the dynamics of individual particles under the tracking control (16). Figure 5 shows individual-particle

dynamics in a three-particle tracking control system. While the velocity of the center of mass asymptotically tracks the commanded velocity $v_{\text{target}} = 1.5$, the individual particles oscillate.

We use Lyapunov methods to analyze the closed-loop error system. Given the tracking error variables in (12), the state-space model of the closed-loop system under control (16) is given by

$$\dot{e}_{i1} = e_{i2}, \tag{34}$$

$$\begin{aligned} \dot{e}_{i2} = & -\gamma e_{i2} + F_i - \bar{k}_1 \left(\sum_{i=1}^N e_{i1} \right) - \bar{k}_2 \left(\sum_{i=1}^N e_{i2} \right) \\ & + [\sin(v_{\text{target}} t) - \sin(e_{i1} + v_{\text{target}} t)], \end{aligned} \tag{35}$$

where $\bar{k}_1 = k_1/N$, and $\bar{k}_2 = k_2/N$. The system (34) and (35) is linear except for the sinusoidal terms, which can be treated as nonlinear perturbations. Following the analysis of the open-loop system, it can be shown that the linear part of the system (35) is locally asymptotically stable. Then, using robust control techniques [26], we can obtain stability conditions for the closed-loop system. Specifically, if the friction coefficient κ and the particle-interaction parameter γ satisfy

$$\kappa > \frac{1}{-\mu_{N-1}}, \quad \gamma > \frac{v_{\text{target}}}{2(-\mu_{N-1}\kappa - 1)}, \tag{36}$$

where μ_{N-1} is the second largest (nonpositive) eigenvalues of the matrix Q , and the control parameters are chosen to satisfy

$$k_1 > 1, \quad k_2 > \max \left\{ \frac{v_{\text{target}}}{2k_1} - \gamma, 0 \right\}, \tag{37}$$

the equilibrium $(0, 0)$ of the error system for individual particles (34) and (35) is locally asymptotically stable. To illustrate this result, Figure 6 shows individual particle trajectories in a three-particle tracking system.

This result is a sufficient condition for stabilizing individual particles along the commanded trajectories, which is consistent with the physical intuition that individual particles are stabilized in their nominal sliding positions when particle interactions are strong enough such that particle interactions are repulsive and the potential between the particles and the substrate is sufficiently strong to lock the phase variables to their nominal positions. These stabilizing conditions are sufficient and may be conservative.

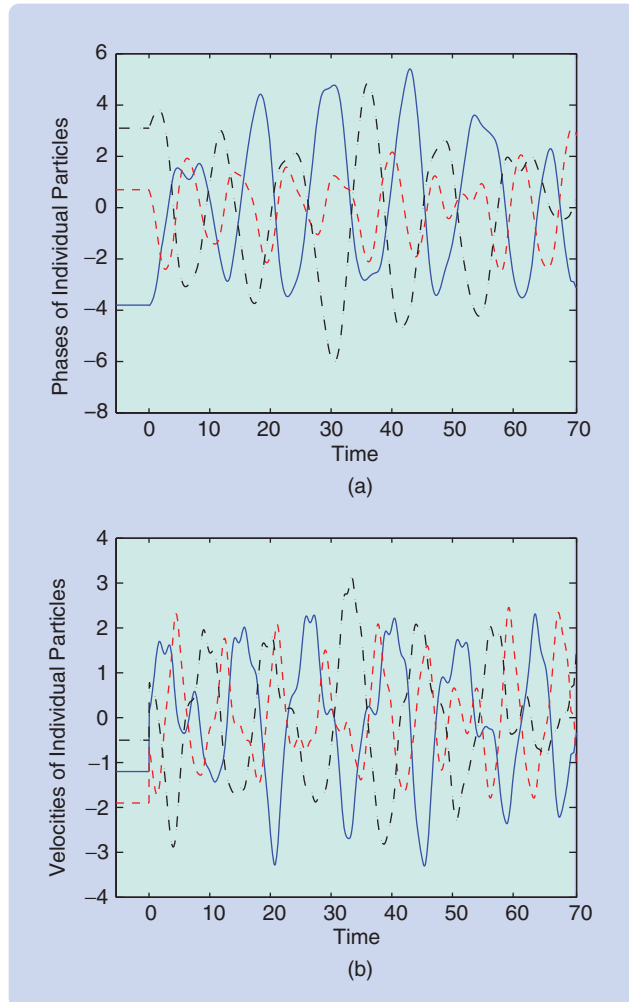


FIGURE 5 Particle dynamics of the average system tracking the commanded average velocity $v_{\text{target}} = 1.5$. (a) The phase variables of individual particles and (b) the velocities of individual particles. The dynamics of each particle oscillate, although the averaged system is Lyapunov stable.

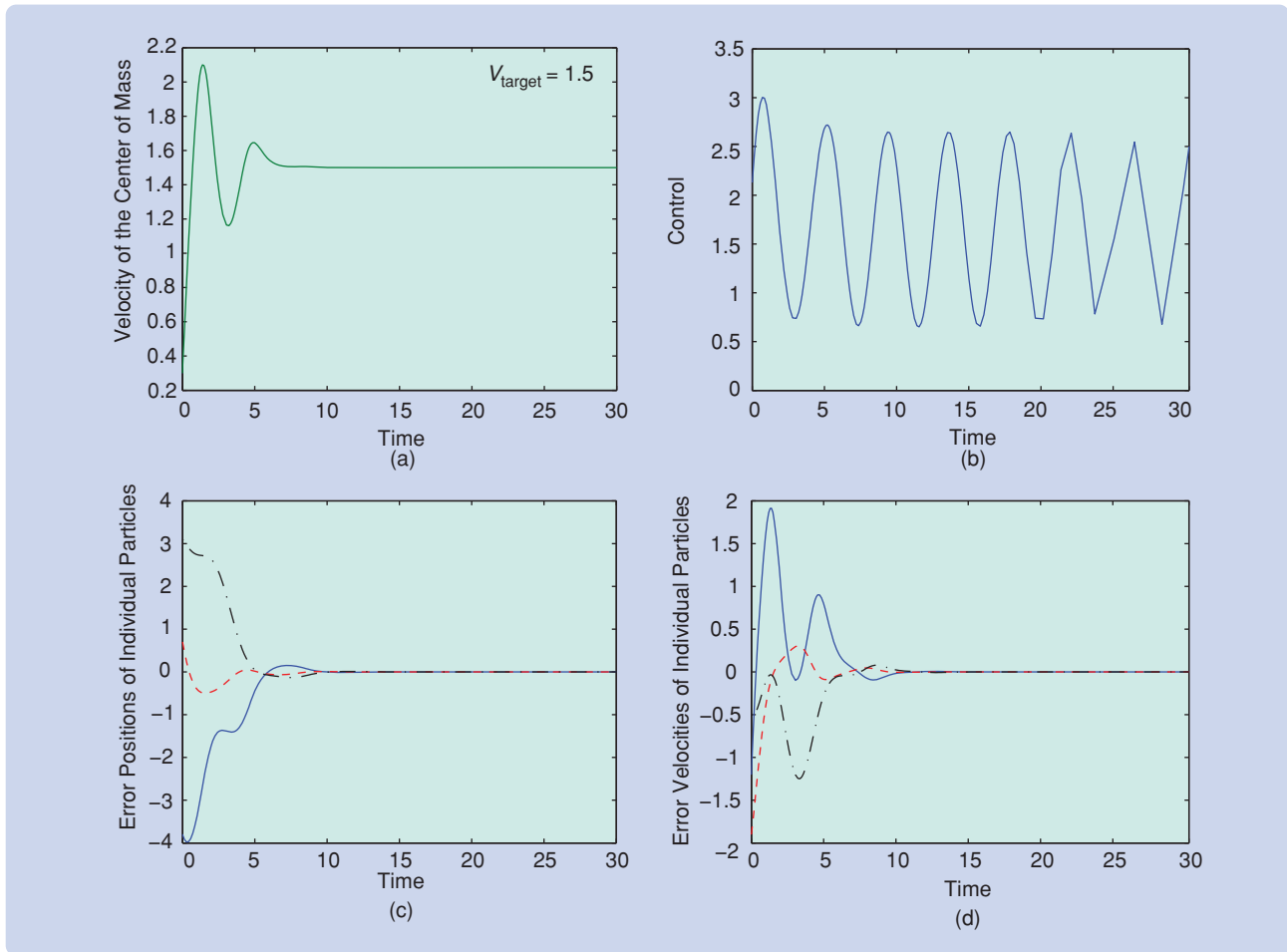


FIGURE 6 Tracking performance of single particles in a three-particle system. The commanded value is $v_{\text{target}} = 1.5$. The system parameters are $\gamma = 1.6$, $\kappa = 1.5$, while the control parameters are $k_1 = 1.2$, $k_2 = 0.4$. (a) The time history of the velocity of the center of the mass, (b) the control history, (c) the error variables between commanded positions and particle positions, and (d) shows the error variables between commanded velocities and particle velocities.

CONCLUSIONS

In this article, motion control in the presence of friction at the nanoscale has been studied using the Frenkel-Kontorova model. Two feedback control design methods have been presented, namely, non-Lipschitzian control and Lyapunov-based control. These control algorithms can be directly applied to quartz-crystal microbalance experiments. For atomic force microscopy and surface-force apparatus experiments, a modification of the algorithms can reduce friction forces. In addition to the analysis of average friction quantities, individual particle motions in both open- and closed-loop systems have been investigated. Under additional conditions on the system parameters, individual particles can also be stabilized. Future research is needed on experimental implementation and testing of these control algorithms.

ACKNOWLEDGMENTS

Yehuda Braiman, Zhenyu Zhang, and Jacob Barhen would like to acknowledge the support by the U.S. Department of Energy, Grant DE-FG02-03ER46091 (Zhenyu Zhang), and the

Division of Materials Sciences and Engineering, Office of Basic Energy Sciences, under contract DE-AC05-00OR22725 with Oak Ridge National Laboratory, managed and operated by UT-Battelle, LLC. Yehuda Braiman would also like to acknowledge the support of the Office of Naval Research.

REFERENCES

- [1] B.N.J. Persson, *Sliding Friction*, 2nd ed. New York: Springer-Verlag, 2000.
- [2] A. Cochard, L. Bureau, and T. Baumberger, "Stabilization of frictional sliding by normal load modulation: A bifurcation analysis," *Trans. ASME*, vol. 70, pp. 220–226, 2003.
- [3] J.P. Gao, W.D. Luedtke, and U. Landman, "Friction control in thin-film lubrication," *J. Phys. Chem. B*, vol. 102, pp. 5033–5037, 1998.
- [4] M. Heuberger, C. Drummond, and J.N. Israelachvili, "Coupling of normal and transverse motions during frictional sliding," *J. Phys. Chem. B*, vol. 102, pp. 5038–5041, 1998.
- [5] M.G. Rozman, M. Urbakh, and J. Klafter, "Controlling chaotic friction," *Phys. Rev. E*, vol. 57, pp. 7340–7443, 1998.
- [6] V. Zaloj, M. Urbakh, and J. Klafter, "Modifying friction by manipulating normal response to lateral motion," *Phys. Rev. Lett.*, vol. 82, pp. 4823–4826, 1999.
- [7] Z. Tshiprut, A.E. Filippov, and M. Urbakh, "Tuning diffusion and friction in microscopic contacts by mechanical excitations," *Phys. Rev. Lett.*, vol. 95, pp. 016101, 2005.

- [8] A. Socoliuc, E. Gnecco, S. Maier, O. Pfeiffer, A. Baratoff, R. Bennewitz, and E. Meyer, "Atomic-scale control of friction by actuation of nanometer-sized contacts," *Science*, vol. 313, pp. 207–210, 2006.
- [9] S. Jeon, T. Thundat, and Y. Braiman, "Effect of normal vibration on friction in the atomic force microscopy experiment," *Appl. Phys. Lett.*, vol. 88, no. 1, pp. 214102.1–214102.3, 2006.
- [10] C.M. Mate, G.M. McClelland, R. Erlandsson, and S. Chiang, "Atomic-scale friction of a tungsten tip on a graphite surface," *Phys. Rev. Lett.*, vol. 59, pp. 1942–1945, 1987.
- [11] S. Fujisawa, E. Kishi, Y. Sugawara, and S. Morita, "Lateral force curve for atomic force/lateral force microscope calibration," *Appl. Phys. Lett.*, vol. 66, pp. 526–528, 1995.
- [12] X. Yang and S.S. Perry, "Friction and molecular order of alkanethiol self-assembled monolayers on Au(111) at elevated temperatures measured by atomic force microscopy," *Langmuir*, vol. 19, pp. 6135–6139, 2003.
- [13] S. Jeon, T. Thundat, and Y. Braiman, "Frictional dynamics at the atomic scale in presence of small oscillations of the sliding surfaces," in *Superlubricity*, A. Erdemir and J.M. Michel, Eds. Amsterdam, The Netherlands: Elsevier, 2007, pp. 119–129.
- [14] Y. Braiman, F. Family, H.G.E. Hentschel, C. Mak, and J. Krim, "Tuning friction with noise and disorder," *Phys. Rev. E*, vol. 59, pp. R4737–R4740, 1999.
- [15] J.P. Gao, W.D. Luedtke, and U. Landman, "Structures, solvation forces and shear of molecular films in a rough nano-confinement," *Tribology Lett.*, vol. 9, pp. 3–13, 2000.
- [16] M. Urbakh, J. Klafter, D. Gourdon, and J. Israelachvili, "The nonlinear nature of friction," *Nature*, vol. 430, pp. 525–528, 2004.
- [17] S.P. Bhat and D.S. Bernstein, "Finite-time stability of continuous autonomous systems," *SIAM J. Contr. Optim.*, vol. 38, no. 3, pp. 751–766, 2000.
- [18] O.M. Braun and Y.S. Kivshar. *The Frenkel-Kontorova Model: Concepts, Methods, and Applications*. Berlin, Germany: Springer-Verlag, 2004.
- [19] Z. Suo and Z. Zhang, "Epitaxial films stabilized by long-range forces," *Phys. Rev. B*, vol. 5, no. 8, pp. 5116–5120, 1998.
- [20] Y. Braiman, J. Barhen, and V. Protopopescu, "Control of friction at the nanoscale," *Phys. Rev. Lett.*, vol. 90, no. 9, pp. 094301.1–094301.4, 2003.
- [21] Y. Guo, Z. Qu, and Z. Zhang, "Lyapunov stability and precise control of the frictional dynamics of a one-dimensional nanoarray," *Phys. Rev. B*, vol. 73, no. 9, pp. 094118.1–094118.5, 2006.
- [22] J. Barhen, S. Gulati, and M. Zak, "Neural learning of constrained nonlinear transformations," *IEEE Computer*, vol. 22, no. 6, pp. 67–76, 1989.
- [23] M. Zak, J. Zbilut, and R. Meyers, *From Instability to Intelligence*. Berlin, Germany: Springer-Verlag, 1997.
- [24] S.P. Bhat and D.S. Bernstein, "Continuous finite-time stabilization of the translational and rotational double integrators," *IEEE Trans. Automat. Contr.*, vol. 43, no. 5, pp. 678–682, 1998.
- [25] H. Khalil. *Nonlinear Systems*, 3rd ed. Englewood Cliffs, NJ: Prentice-Hall, 2002.
- [26] Z. Qu, *Robust Control of Nonlinear Uncertain Systems*. New York: Wiley, 1998.
- [27] Y. Guo and Z. Qu, "Control of frictional dynamics of a one-dimensional particle array," *Automatica*, vol. 44, no. 10, pp. 2560–2569, 2008.
- [28] J.J.E. Slotine and W. Li, *Applied Nonlinear Control*. Englewood Cliffs, NJ: Prentice-Hall, 1991.
- [29] C. Godsil and G. Royle, *Algebraic Graph Theory*. New York: Springer-Verlag, 2001.
- [30] C.W. Wu, *Synchronization in Coupled Chaotic Circuits and Systems*. Singapore: World Scientific, 2002.

AUTHOR INFORMATION

Yi Guo (yguo1@stevens.edu) received the Ph.D. degree from the University of Sydney, Australia, in 1999. She is an assistant professor in the Department of Electrical and Computer Engineering at Stevens Institute of Technology. Prior to joining Stevens in 2005, she was a visiting assistant professor in the Department of Electrical and Computer Engineering at University of Central Florida. From 2000 to 2002, she was a research fellow in the Computer Science and Mathematics Division of Oak Ridge National Laboratory. Her research interests include nonlinear control,

mobile robotic systems, cooperative and decentralized control, and control applications. She is a Senior Member of the IEEE. She can be contacted at the Department of Electrical and Computer Engineering, Stevens Institute of Technology, Hoboken, NJ 07030 USA.

Zhihua Qu received the Ph.D. degree in electrical engineering from the Georgia Institute of Technology in 1990. Since then, he has been with the University of Central Florida, where he is a professor in the School of Electrical Engineering and Computer Science. His research interests include nonlinear systems and control, cooperative control, robust and adaptive control designs, and robotics. He is the author of two books, *Robust Control of Nonlinear Uncertain Systems* and *Robust Tracking Control of Robotic Manipulators*. He is an associate editor for *Automatica* and the *International Journal of Robotics and Automation*.

Yehuda Braiman received the Ph.D. from the Tel Aviv University in 1993. He is a senior research staff member at the Center for Engineering Science Advanced Research, Computer Science and Mathematics Division at the Oak Ridge National Laboratory (ORNL). Previously, he was a visiting assistant professor at Emory University and a post-doctoral fellow at Georgia Institute of Technology and at Emory University. His research interests include modeling fracture propagation in metallic glasses, friction and control of friction at the atomic scale, coherent beam combining of arrays of high power semiconductor lasers, and nonlinear dynamical systems. He is a member of the APS and MRS.

Zhenyu Zhang received the Ph.D. degree in condensed matter theory from Rutgers University in 1989. He is a distinguished research scientist in the Materials Science and Technology Division of Oak Ridge National Laboratory and professor of physics at the University of Tennessee. His research focuses on the theoretical understanding of the formation, stability, properties, and potential applications of low-dimensional materials. He is a fellow of the American Physical Society and is on the editorial boards of *Physical Review Letters*, *Chinese Physics Letters*, and *ACTA PHYSICA SINICA*.

Jacob Barhen is a UT-Battelle Corporate Fellow and, since 1994, director of the Center for Engineering Science Advanced Research at the Oak Ridge National Laboratory. From 1987 to 1994, he was the head of the Neural Computation and Nonlinear Science Group at Caltech/JPL. His research interests include emerging computational systems, global optimization, sensitivity and uncertainty analysis, neural networks, and signal processing. He has received three NASA Space Act awards for contributions to the National Space Program, 11 NASA awards for technical innovation, and an R&D-100 award. He is a member of the editorial boards of the *International Journal of Distributed Sensor Networks*, *Neural Processing Letters*, *Neural Networks*, *Mathematical and Computer Modeling*, and *Concurrency and Computation*. He received the Ph.D. from the Technion–Israel Institute of Technology in 1978. 